Journal of Ovonic Research Vol. 11, No. 6, November - December 2015, p.271 - 276

MECHANICAL FABRICATION AND CHARACTERIZATION OF ZINC OXIDE (ZnO) NANOPARTICLES

K. K. TAHA[a, c], M. O. M'HAMED[a], H. IDRISS[b,d]
[a]*Dept. of Chem., College of Science, AI Imam Mohammad Ibn Saud Islamic University (IMSIU), P.O. box : 5701, Riyadh, KSA*
[b]*Committee on Radiation and Environmental Pollution Protection, College of Science, AI Imam Mohammad Ibn Saud Islamic University (IMSIU), P.O. box : 5701, Riyadh, KSA*
[c]*Dept. of Chem. & Ind. Chem., College of Science, University of Bahri, Khartoum, Sudan*
P.O. box : 5701, Riyadh, KSA
[d]*Sudan Atomic Energy Commission, Khartoum, Sudan*

In this work, we present fabrication and characterization of zinc oxide (ZnO) nanoparticles with crystallite sizes from 26 nm to 22 nm. Commercial ZnO powders were subjected to milling in a high energy ball mill for different time intervals: 2, 4, 6 and 12 hours. Crystal structure of the ZnO nanoparticles was studied by X-ray diffraction(XRD) technique. From the X-ray patterns, Scherer equation was used for nanoparticles sizes determination. On the other hand, crystal lattice parameters of the hexagonal ZnO were also calculated. Thermogravimetric analysis has revealed that less weight was lost in the milled samples.

(Received September 7, 2015; Accepted November 9, 2015)

Keywords: ZnO nanoparticles, fabrication , XRD , Thermogravimetric , Crystal structure

1. Introduction

The unique and interesting properties of nanomaterials have motivated the researchers to adopt and develop simple, inexpensive techniques to synthesize nanostructures for application as advance technological materials [1]. Zinc nanomaterials show varying optical and electrical properties that depend mainly on size and shape [2]. Due to its wide band gap (3.37 eV), ZnO nanoparticles find interesting applications as photonic and electronics materials. Very small size ZnO nanoparticles exhibit quantum confinement effect that render them useful in many applications such as gas sensing, optoelectronic devices [3,4,5]. Many techniques have been employed in ZnO nanoparticles synthesis including sol-gel, hydrothermal, chemical vapour deposition, electrochemical and sonochemical methods [6,7]. Ball milling is a simple, inexpensive and effective technique for synthesis of nanomaterials [8,9]. In literature there are studies of utilizing ball milling to synthesize TiO2 nanoparticles nanotubes of boron and carbon, ZnO nanoparticles [10,11,12]. The melting point of nanomaterials is lowered due to balling milling process and hence synthesis at low temperature is achieved. Thus we can synthesize nanomaterials at ambient temperature to avoid high energy consumption, organic solvents and gaseous emissions. Moreover long time for processing of the nanomaterials can be saved beside the high safety attained [13]. Obviously ball milling brings changes in the morphology and structure of nanoparticles, still optical and electrical properties are altered[14].

*Corresponding author: kamaltha60@gmail.com

2. Experimental

The starting material was commercial ZnO of high purity. The milling was carried out for the dry sample in Planetary Micro Mill PULVEISETTE 7 at 200 rpm for 2, 4 and 6 hours at 1:10 powder to ball ratio. An extreme condition of 12 hours time interval and 1:20 powder to ball mass ratio at 400 rpm was carried out also. No further process was done for the ball milled product. Powder XRD measurements were performed using the X-ray diffractometer (Shimadzu XD-3A) in the diffraction angle range $20° \leq 2\Theta \leq 80°$, with monochromatic Cu K radiation (($\lambda = 1.5406$ A°) source. Thermal gravimetric analysis (TGA) was carried out using Mettler Toledo microbalance. Approximately 20mg of the sample is placed in a platinum crucible on the pan of the microbalance and heated from room temperature to 1000°C, using Al_2O_3 as inert material. Analysis was performed under nitrogen flow at heating rate of $10°C/min^{-1}$.

3. Results and discussion

Typical XRD patterns of ZnO nanoparticles before and after milling are shown in Fig. 1. The diffraction peaks at angles 2Θ of 31.34°, 34.39°, 36.23°, 47.51°, 56.56°, 62.56°, 66.29°, 67.66° and 68.81° correspond to the reflection from the (1 0 0), (0 02), (1 01), (1 0 2), (11 0), (1 03), (2 0 0) and (112) crystal planes of the hexagonal wurtzite zinc oxide structure (JCPDS 36-1451) can be seen at the spectrum of the ZnO before milling. After milling the main peaks have shifted to higher values with increase in time (see table 1). Such increase in 2Θ is an indication of a strain in the sample after milling. Some previous reports have shown that the intrinsic strain in ZnO samples is attributed to the deficiency of crystallites as a result of milling [15]. The broadening of the XRD line for the milled nanoparticles, as shown in Fig. 1, may be attributed to the reduction in particle/crystallite size and strain induced by the milling process [16]

Table (1): 2 theta values for pure and milled ZnO nanoparticles

Planes (hkl)	**0 hour**	**2 hours**	**4 hours**	**6 hours**
	2θ°			
100	31.34	31.89	31.60	32.02
002	34.39	34.58	34.45	34.45
101	36.232	36.298	36.33	36.45
102	47.51	47.549	47.41	47.53
110	56.56	56.82	56.53	56.56
103	62.56	62.94	62.83	62.82
200	66.29	66.49	66.21	66.23
112	67.66	68.07	67.9	67.94
201	68.81	69.05	69.21	69.27

The lattice constant *a* for the plane $\langle 100 \rangle$ was calculated using the formula [17]

$$a = \frac{\lambda}{\sqrt{3} Sin\theta}$$

While the other lattice constant c was obtained by [17]

$$c = \frac{\lambda}{Sin\theta}$$

The crystallite sizes of the ZnO nanoparticles (D) can be obtained using Scherer equation, $D = \frac{k\lambda}{B_{hkl}\cos\theta}$ [18], where D is the thickness of (hkl) crystal plane, k is the wavelength of the incident X-ray (1.5406 A°) for Cu Kα, k is a constant equal to 0.90 [11], B_{hkl} is the peak width at half-maximum intensity, and Θ is the peak position. The (101) plane (the strongest) was selected to calculate the crystallite size. As can be seen from Table 2, the particle size decreased as the milling time was increased.

Table (2): The lattice constant values for the samples at different milling time

Sample	a	c	c/a	D (nm)	strain	δ (nm)$^{-2}$
0 hour	3.28	5.211	1.589	200		
2 hours	3.22	5.1907	1.612	27.13	0.0081	13.58 x 10^{-4}
4 hours	3.24	5.2030	1.601	25.70	0.0085	15.14 x 10^{-4}
6 hours	3.26	5.2188	1.600	23.79	0.0093	17.67 x 10^{-4}

The lattice parameters are shown in table (2). The lattice parameter a and c have reduced after the milling process. The values for the lattice parameters a and c are identical to those reported [19] for ZnO nanopaticles prepared by ball milling. The lattice parameters obtained in this work highly match with the those previously reported [20].

The d-spacing was calculated by both using the Bragg law $d = \frac{\lambda}{2Sin\theta}$ as well as the formula: $\frac{1}{d^2_{(hkl)}} = \frac{4}{3}\left(\frac{h^2+hk+k^2}{a^2}\right)+\frac{l^2}{c^2}$ that relates it to the lattice constants. The values obtained were almost similar (Table 3). It can also be observed that there is a decrease of interplanar spacing (d).

Table (3): The d_{hkl} for the samples at different milling time intervals from experimental and theoretical calculations

Sample	d (Bragg)	d (formula)	% Reduction
0 h	2.4754	2.5017	
2 h	2.4632	2.4566	0.49
4 h	2.4695	2.4697	0.23
6 h	2.4639	2.4632	0.46

The dislocation density (δ), that indicates the amount of defects is defined as the length of dislocation line per unit volume of the crystal, is calculated via the relation[21].

$$\delta = \frac{1}{D^2}$$

The Zn - O bond length L is given by[22].

: $L = \sqrt{\left(\frac{a^2}{3}\right)+\left(\frac{1}{2}-\mu\right)^2 c^2}$, here μ is the measure of an atom displacement to the neighboring one along the "c" axis. The value of μ is calculated by the equation: $\mu = \frac{a^2}{3c^2}+0.25$. The

parameter μ changes inversely with c/a ratio in a way to maintain the tetrahedral dimensions due to the angle distortion. From Table (3), it can be seen that μ decreases with the increase in c/a ratio. On the other hand the L values obtained is almost equal to the 1.9767 Å value reported by Seetawan *et al*. [22].

Table 4. The values of u and L for samples at different milling time intervals

Sample	δ (nm)$^{-2}$	*u*	L (Å)
0 hour		0.3766	1.9792
2 hours	13.58 x 10^{-4}	0.3783	1.9635
4 hours	15.14 x 10^{-4}	0.3796	1.9727
6 hours	17.67 x 10^{-4}	*0.3801*	1.9834

It worth to notice that when the milling was prolonged to 12 hours under high rpm the ZnO has lost its characteristic hexagonal structure (Fig. 2).

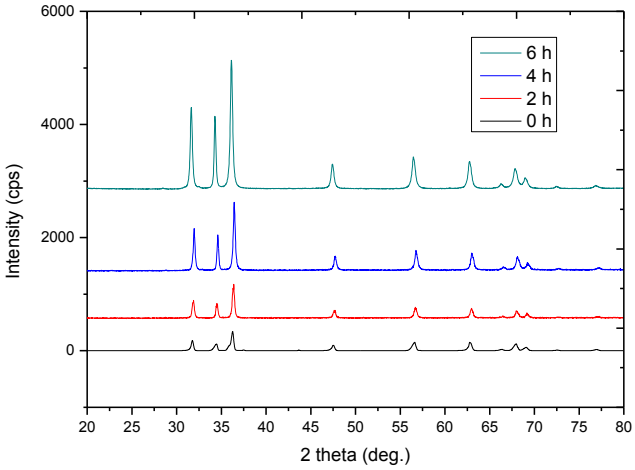

Fig. 1. XRD spectrum of pure and milled ZnO

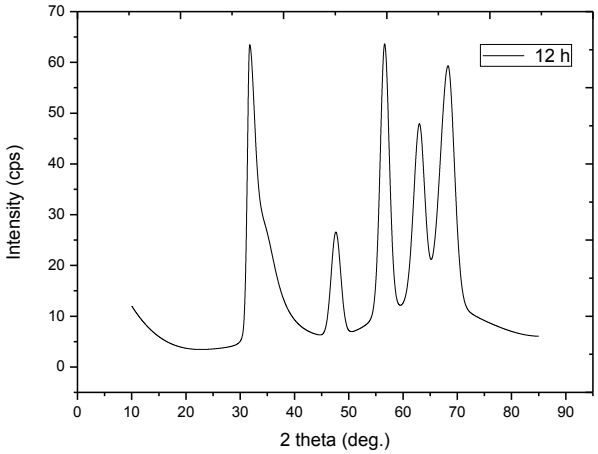

Fig. 2. XRD spectrum of 12 hour milled ZnO

The thermogravimetric (TGA) analysis curves ZnO and ZnO prepared by ball milling are displayed in figure 3 It is clearly seen that the TG curve for milled ZnO does not show any significant weight loss in the studied temperature range. On the contrary there is weight loss at around 40 -100 °C due to water loss along with another weight loss process at 500 - 750 °C in case of raw samples. When the nanomaterial was milled no weight loss was observed indicating an improvement in its stability.

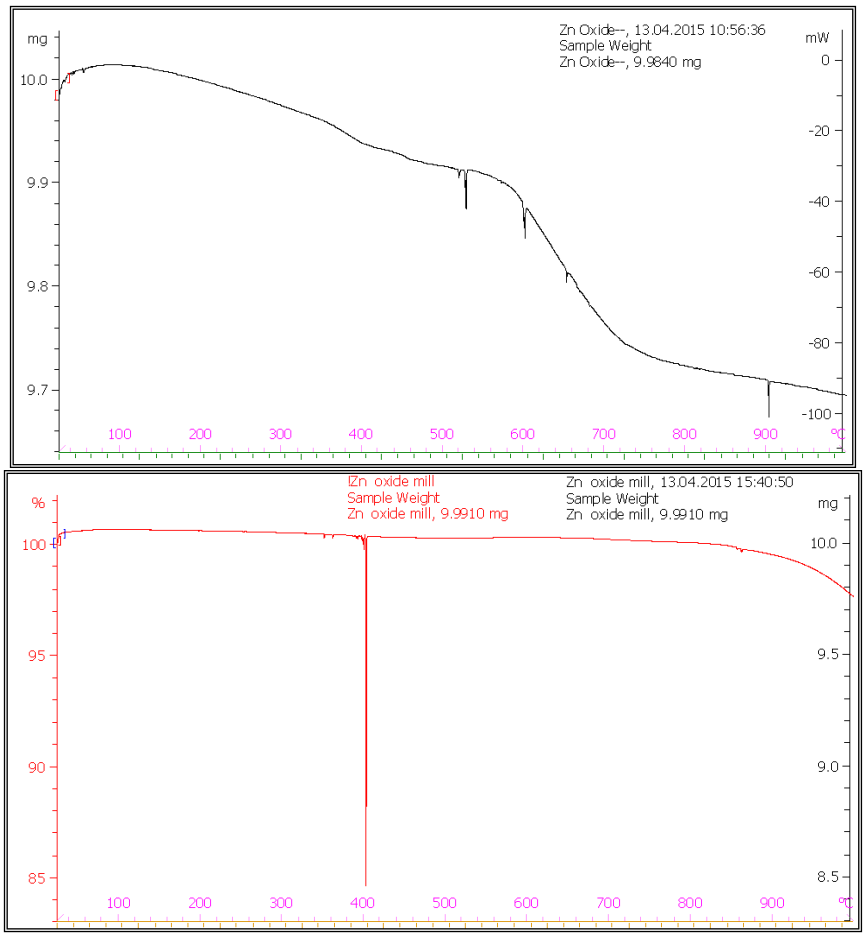

Fig. 3: The TGA of pure ZnO (above) and milled sample (below)

4. Conclusions

Zinc oxide (ZnO) nanoparticles were fabricated from high purity ZnO powder through mechanical milling for different time intervals. The synthesized nanoparticles were analyzed using XRD and TGA analysis. The different lattice parameters were calculated and the results showed a reduction in particle size due to milling. The TGA analysis revealed that highly stable nanoparticles were prepared.

References

[1] M.A. Shah, Al-Shahry, JKAU: Sci., **21**, 61 (2009).
[2] R. E. Smalley, B. I. Yakobson Solid State Communications, **107**(11), 597 (1988).
[3] R. Paneva, D. Gotchev, Sensors and Actuators A: Physical, **72**(1), 79 (1999).
[4] N. T. Hung, N. D. Quang, S. Bernik J. Material Research. **16**(10), 2811823(2001).
[5] L Zhao, PF Lu, ZY Yu, XT Guo, Y Shen, H Ye, GF Yuan, L Zhang: J Appl Phys,

108, 113924 (2010).
[6] M. Darroudi, Z. Sabouric, R. K. Oskuee, A. K. Zake, H. Kargarc, M. H. N. A. Hamid Ceramic Int., **39**, 9195 (2013).
[7] A. khorsandzak, W. H. abd Majid, H. Z. Wang, Ramin Yousefi, A. Moradi Golsheikh, N. Z. Ren, Ultrasonic Sonochemistry, **20**, 395 (2013).
[8] A. S. Bolokang, F. R. Cummings, B. P. Dhonge, H. M. I. Abdallah, T. Moyo, H. C. Awart, C. J. Arendse, T. F. G. Muller and D. E. Motaung, Applied Surface Science,**331**; 362 (2015).
[9] Y. Chen, J. F. Gerald, J. S. Williams and P. Willis, Journal of Metastable and Nanocrystalline Materials, **2-6**, 173 (1999).
[10] Y. Chen, M.J. Conway, J.D. Fitzgerald, Applied Physics A: Materials Science &Processing, **76**, 633 (2003).
[11] L.C. Damonte, L.A. Mendoza Zelis, B. Marı Soucase, M.A. Hernandez Fenollosa Powder Technology, **148,** 15 (2004).
[12] J. S. Lee, K. Park, M. I. Kang, I. W. Park, S. W. Kim, W. K. Cho, H. S. Han, S. Kim, Journal of Crystal Growth , **254**(3-4); 423 (2003).
[13] Q. Li, C. Liu, Z. Liu, Q. Gong, Optics Express **13**(6), 1833 (2005).
[14] P. K. Giri, S. Bhattacharyya, D. K. Singh R. Kesavamoorthy, B. K. Panigrahi, K. G. M. Nair. Journal Of Applied Physics **102**, 093515 (2007).
[15] L. C. Damonte, L. A. M. Zelis, B. M. Soucase, and M. A. H. Fenollosa, Powder Technol. **148**; 15 (2004).
[16] B. D. Cullity, S. R. Stock, Elements of X-ray diffraction. 3rd edn, Prentice Hall, New Jersey (2001)
[17] A. Khorsand Zak, W.H.Abd. Majid, M.E. Abrishami, R. Yousefi, Solid State Sciences **13,** 251 (2011)
[18] A.L. Patterson, Physical Review **56,** 978 (1939).
[19] N. Salah, S. S. Habib, Z. K. Khan, A. Memic, A. Azam, E/ Alarai, N. Zahed, S. Al-hamedi. Int J Nanomedicine. **6**, 863 (2011).
[20] M. Saleem, L. Fang, H. B. Ruan, F. Wu, Q. L. Huang, C. Y. Kong, Intl. J. Phy. Sci., **7**(23), 2971 (2012)
[21] C. S. Barret, T. B. Massalski Structure of Metals. Pergamon Press, Oxford (1980)
[22] U. Seetawan, S. Jugsujinds, T. Seetawan, A. Ratchasin, C. Euvanaont, C. Junin, C. Thanachayanont, P. Chainaronk, Maters Sci. Appls, **2**; 1302 (2011).